

RESEARCH

Open Access



Three-dimensional analysis of the relationship between mandibular retromolar space and positional traits of third molars in non-hyperdivergent adults

Yumei Huang^{1,2,3}, Yunjia Chen^{1,2,3}, Dan Yang^{1,2,3}, Yingying Tang^{1,2,3}, Ya Yang^{1,2,3}, Jingfeng Xu^{1,2,3}, Jun Luo^{1*} and Leilei Zheng^{1,2,3*}

Abstract

Background The anatomical position of the mandibular third molars (M3s) is located in the distal-most portions of the molar area. In some previous literature, researchers evaluated the relationship between retromolar space (RS) and different classifications of M3 in three-dimensional (3D) cone—beam computed tomography (CBCT).

Methods Two hundred six M3s from 103 patients were included. M3s were grouped according to four classification criteria: PG-A/B/C, PG-I/II/III, mesiodistal angle and buccolingual angle. 3D hard tissue models were reconstructed by CBCT digital imaging. RS was measured respectively by utilizing the fitting WALA ridge plane (WP) which was fitted by the least square method and the occlusal plane (OP) as reference planes. SPSS (version 26) was used to analyze the data.

Results In all criteria evaluated, RS decreased steadily from the crown to the root ($P < 0.05$), the minimum was at the root tip. From PG-A classification, PG-B classification to PG-C classification and from PG-I classification, PG-II classification to PG-III classification, RS both appeared a diminishing tendency ($P < 0.05$). As the degree of mesial tilt decreased, RS appeared an increasing trend ($P < 0.05$). RS in classification criteria of buccolingual angle had no statistical difference ($P > 0.05$).

Conclusions RS was associated with positional classifications of the M3. In the clinic, RS can be evaluated by watching the Pell&Gregory classification and mesial angle of M3.

Keywords Retromolar space, M3 positional traits, The fitting WALA ridge plane, Occlusal plane

*Correspondence:

Jun Luo

500210@hospital.cqmu.edu.cn

Leilei Zheng

zhengleileicqmu@hospital.cqmu.edu.cn

Full list of author information is available at the end of the article



© The Author(s) 2023. **Open Access** This article is licensed under a Creative Commons Attribution 4.0 International License, which permits use, sharing, adaptation, distribution and reproduction in any medium or format, as long as you give appropriate credit to the original author(s) and the source, provide a link to the Creative Commons licence, and indicate if changes were made. The images or other third party material in this article are included in the article's Creative Commons licence, unless indicated otherwise in a credit line to the material. If material is not included in the article's Creative Commons licence and your intended use is not permitted by statutory regulation or exceeds the permitted use, you will need to obtain permission directly from the copyright holder. To view a copy of this licence, visit <http://creativecommons.org/licenses/by/4.0/>. The Creative Commons Public Domain Dedication waiver (<http://creativecommons.org/publicdomain/zero/1.0/>) applies to the data made available in this article, unless otherwise stated in a credit line to the data.

Background

Molar distalization (MD) is a method for extending the length of dental arch [1]. Particularly in recent years, due to the popularity of invisible orthotics, the realization rate of molar distal movement has been greatly improved [2, 3]. In the orthodontic clinic, orthodontists always relieve mild or moderate crowding and adjust the molar position relationship by MD [4, 5]. At this time, the question arises of where the boundary of the tooth movement is.

The limit of MD depends on the determination of alveolar bone anatomical limit. The maxillary arch incorporates a clear posterior limit—the maxillary tuberosity [6, 7]. Hence, MD is commonly utilized within the orthodontic process of the maxillary dentition. The conventional way of MD mostly uses the skeletal anchorage system, face-bow, and temporary skeletal anchorage devices, all of these can accomplish certain effect [8, 9].

The mandible is composed of mandibular body and mandibular ramus. It is a complex structure, with masticatory muscles attached and high bone density. MD in mandible is difficult. With the popularity of cone-beam computed tomography (CBCT), increasingly scholars have studied MD in mandible.

Kim [10] selected the normodivergent facial type of patients to study and proposed that the farthest lingual cortical bone of the mandibular arch was the posterior anatomical boundary and found the RS had the minimum at the root tip. In orthodontics, vertical facial types include hypodivergent, normodivergent and hyperdivergent types. We selected patients with non-hyperdivergent adults, including hypodivergent and normodivergent patients. Choi et al. found that RS did not differ significantly between class I and class III malocclusion [11]. But in previous studies, the anatomic characteristics of the mandibular angle related to MD were not considered. Third molars (M3s) are the distal structure of the mandibular dental arch, located at the turning point of the mandibular body and ramus. It has been reported that the positional traits of M3s can affect the anatomical relationship of the transition area to a certain extent [12]. The shape, position and inclination of M3s are regularly utilized to assess the difficulty of the extraction of M3 in maxillofacial surgery [13].

Be that as it may, the relationship between distinctive positional sorts of M3 and RS has not been thoroughly analyzed. The purpose of this study is to quantitatively measure RS of the mandible with CBCT, and test for an association between RS and positional traits of the M3, so as to assist orthodontists design treatment plans.

Materials and methods

Sample selection

This study was approved by the Research and Ethics Committee of the Affiliated Stomatology Hospital of Chongqing Medical University (CQHS-REC-2021(LSNo.045)).

The sample included CBCT imaging of 103 subjects (52 males and 51 females, mean age = 28.39 years, 206 M3), aged from 18 to 40 years. These subjects were selected from the patients who were admitted for orthodontic treatment from 2019 to 2021 at the Department of Orthodontics, Affiliated Stomatology Hospital of Chongqing Medical University. The CBCT in this study was taken due to the patient's need to have the M3 removed and was taken prior to orthodontic treatment.

The inclusion criteria: (1) non-vertical facial dimension ($SN-MP^\circ < 32^\circ$) and Class I or Class III malocclusion, (2) normal overjet and overbite, (3) crowding of less than 4 mm in the mandibular dental arch, (4) no significant alveolar bone loss, (5) no missing teeth in mandible (including M3s), (6) no noticeable facial asymmetry and deformation, (7) no tumors, fractures, cysts in mandible, (8) no diagnosed systemic disease, (9) no history of orthodontic treatment.

The exclusion criteria: (1) blurred CBCT imaging, (2) incomplete CBCT imaging, (3) unmeasurable CBCT imaging.

Construction of 3D models, reference planes and measuring lines

CBCT images (KaVo Dental GmbH, USA; 80 mA, 80 kVp, and 8.9-s scan time) were procured. The data was imported into Mimics 19.0 software (Materialise, Leuven, Belgium) in Digital Imaging and Communications in Medicine (DICOM) format to reconstruct the 3D hard tissue models (Fig. 1A). Connecting the left and right orbital points (Or-R, Or-L) and the right porion point (Po-R) as the Frankfort horizontal plane (FH). Connecting two mesiobuccal cusp points of the mandibular first molars (L6R-MB, L6L-MB) and the mesial contact point of the lower central incisor (LIE) as occlusal plane (OP) (Fig. 1B).

We constructed a new plane as a reference plane, which was a plane fitted by the most prominent bony WALA point at the boundary of the basal bone arch just below 14 mandibular teeth. We got the coordinate points of bony WALA ridge in Mimics software and imported the coordinate values into Matlab software (R2022a, MathWorks, U.S) [14] to complete the fitting of WP, and finally imported WP into Mimics. The process was shown in Fig. 2.

To construct the reference lines. Connecting the bone marker points of the WALA ridge of the mandibular

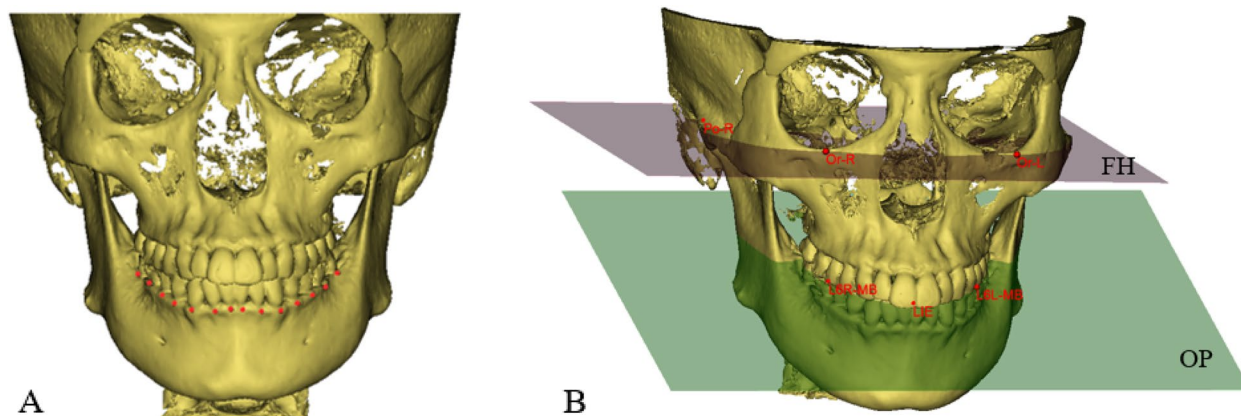


Fig. 1 Construction of 3D model, reference plane. **A** 3D hard tissue model and bone marker points of mandibular WALA ridge. **B** The Frankfort horizontal plane (FH) and the occlusal plane (OP)

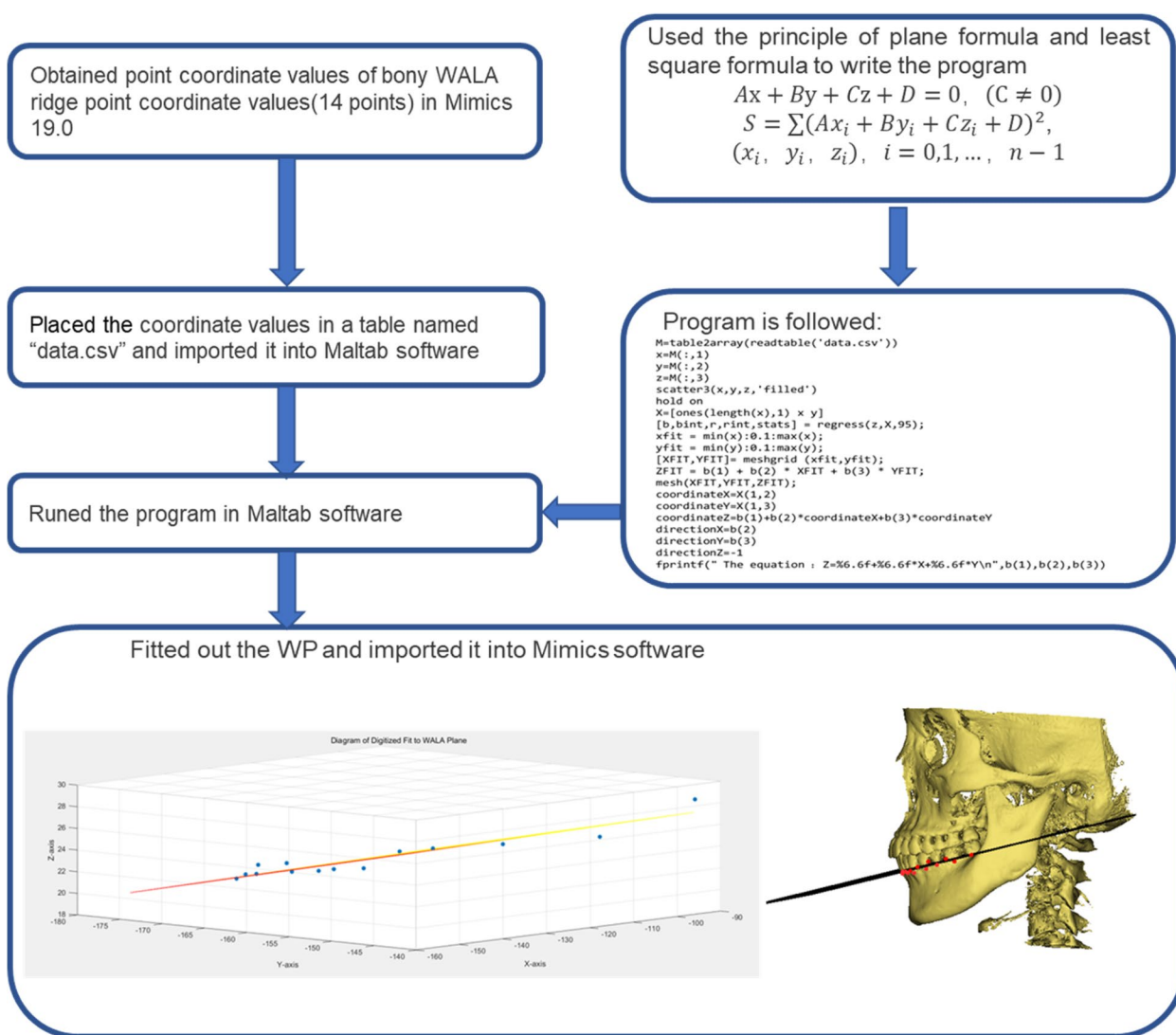


Fig. 2 The process of complete the fitting of WP

first and second molar as the WALA ridge line (WL) (Fig. 3A). Connecting the mesial buccal cusps of the mandibular first and second molar as the occlusion line (OL) (Fig. 3B).

Variables and measurements

The 3D hard tissue models were imported into the Measure and Analysis Module of Mimics for creating FH, WP, OP, WL, and OL. The angles of FH with WP, WL, OP and OL were respectively recorded as \angle FH-WP, \angle FH-WL, \angle FH-OP, \angle FH-OL. These FH-related angulations

were measured by the projection on the sagittal section (Fig. 3A, Fig. 3B). Recording the mesiodistal angulation (A angle: $-10^\circ \sim 100^\circ$), labiolingual angulation (B angle) of M3 in WP-based and OP-based reference frames, separately. The detailed protocol of CBCT measurements described in Fig. 4.

RS was measured on five different levels which were parallel to the horizontal plane including levels 1–5 in two reference frames (Table 1, Fig. 5A). Levels 1–2 were at the crown level. Levels 3–5 were at the root level. The distance from the distal protruding point of the crown of

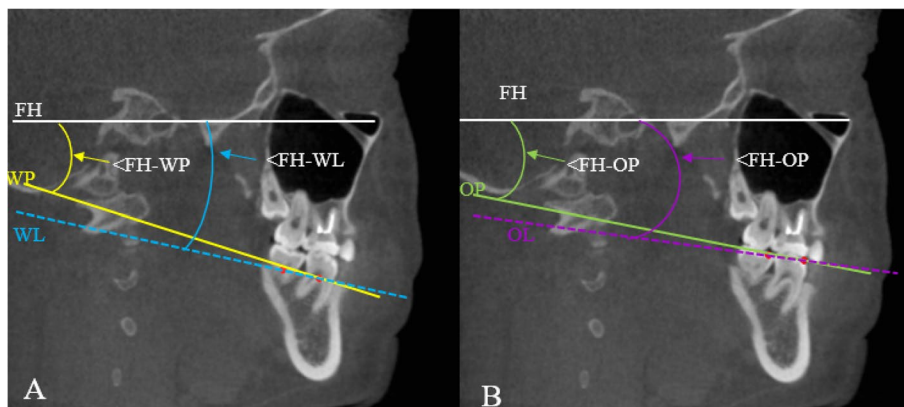


Fig. 3 The projected schematic diagram of reference plane, line and the FH-related angulations on the sagittal plane. **A** FH, WP, WL and the \angle FH-WP, \angle FH-WL. **B** FH, OP, OL and \angle FH-OP, \angle FH-OL

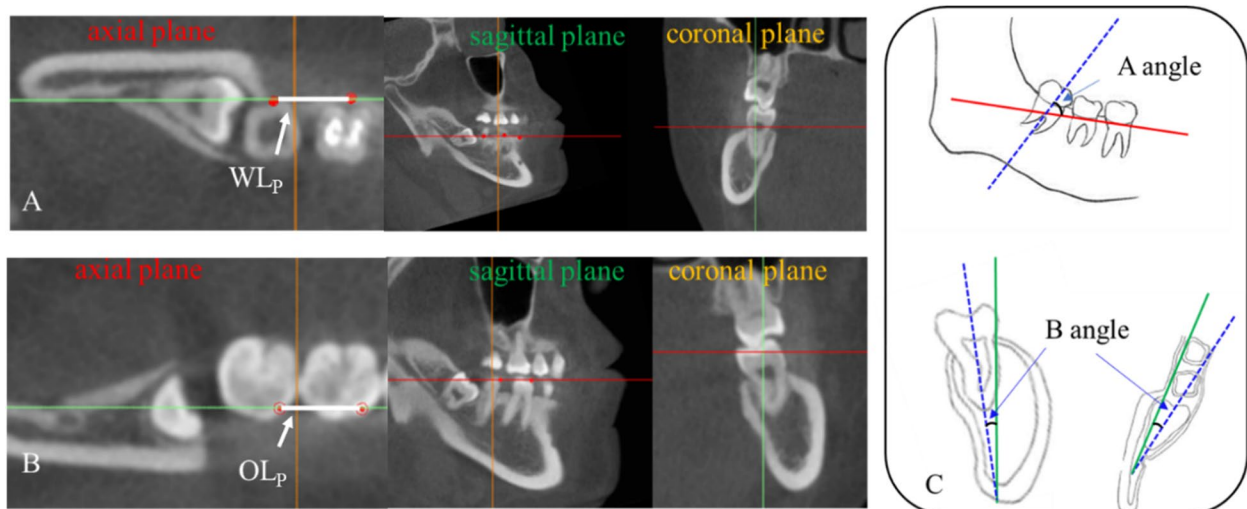


Fig. 4 The detailed protocol of A, B angle measurements. Creating local 3D reference frames, the correlated planes were determined by intersected guidelines with different colors, which were red for axial planes, green for sagittal planes, and orange for coronal planes. **A** WP-based reference frame. Take WP as horizontal plane, project the bony WALA ridge marks of the first and second molars on the horizontal plane, connect the two points as WL_p, make the sagittal plane through WL_p and perpendicular to the horizontal plane, and make the coronal plane through one mark and perpendicular to the horizontal plane and sagittal plane. **B** OP-based reference frame. The method was the same as A, and the two landmarks were replaced by the mesial buccal cusp of the first and the second molars. **C** Mesiodistal angle (A angle): Find the sagittal section of the longest tooth axis of M3 and record the angle between this axis and the horizontal plane in the sagittal plane; labiolingual angle (B angle): Find the coronal or horizontal section of the longest tooth axis of M3, record the angle between this axis and the sagittal plane in the coronal or horizontal plane

Table 1 Explanation the position of five levels

| Level | abbreviation | Interpretation |
|---------|--------------|---|
| Level 1 | L1 | The level parallel to reference plane through the most distal protruding point of the crown of the mandibular second molars |
| Level 2 | L2 | The level parallel to reference plane through the cement enamel-junction of the mandibular second molars |
| Level 3 | L3 | The level parallel to reference plane through the root furcation of the mandibular second molars |
| Level 4 | L4 | The level parallel to reference plane through the distal root of the mandibular second molars |
| Level 5 | L5 | The level parallel to reference plane through the apex of the distal root of the mandibular second molars |

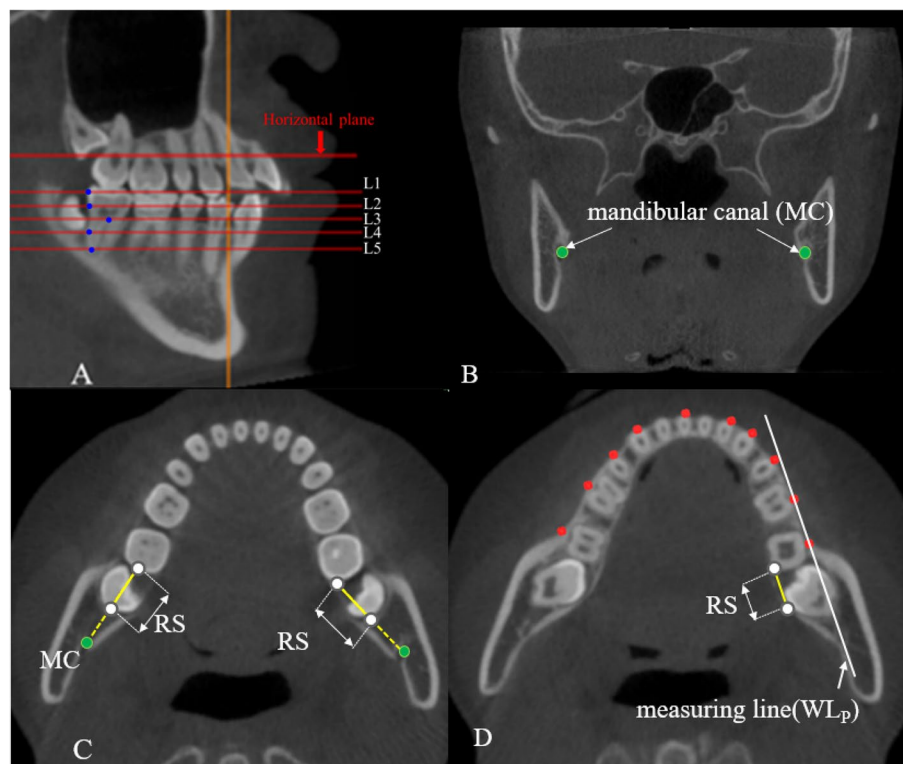


Fig. 5 levels 1–5, mandibular canal and measurements. **A** L1 to L5. **B** the mandibular canal. **C** the measurement diagram of RS in crown level. **D** the measurement diagram of RS in the root level (The measurement method of RS on OP-based level by using OL_p was consistent with this)

the mandibular second molar to the anterior wall of the mandibular canal (MC) (Fig. 5B) was measured as RS at the crown level [15] (Fig. 5C). The distance from the most lingual point of the distal root of the second molar to the lingual cortical bone of the mandible which parallels the measuring line (WL_p or OL_p) was measured as RS at the root level [10] (Fig. 5D). Data obtained by using WP or OP plane as reference plane were recorded as WP group and OP group, respectively.

Classifications and groups of third molars

M3 positional traits and eruption space measurements were recorded on CBCT derived panoramic radiographs.

According to Pell &Gregory classification (Depth: PG-A, PG-B, PG-C; Ramus Relationship: PG-I, PG-II, PG-III) (Fig. 6) [16, 17] and the angles of WP-based reference frame to classify M3s (A angle: [A1:<27°, A2:27~67°, A3:>67°]; B angle: [B1:<14°, B2:14~24°, B3:>24°]). WP-based reference system is the main reference system in this study, and OP-based reference system was used as an auxiliary system. M3s were classified according to the A and B angles of the former. We divided the A angle and B angle into the three classifications according to the trisection of a sample size to ensure the comparability between samples, individually. Additionally, all M3s also were grouped according to the patient’s age, sex, and

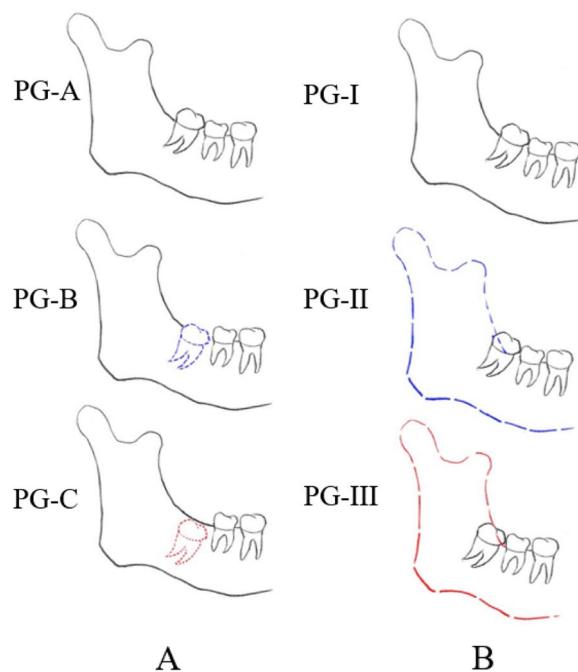


Fig. 6 The classification criterion of Pell&Gregory. **A** Depth of Pell&Gregory Classification. PG-A: The highest part of the M3 was on the same level or higher than the occlusion plane of the second molar. PG-B: The highest part of the M3 is below the occlusal plane of the second molar, but higher than the neck of the second molar. PG-C: The highest position of the M3 is below the neck of the second molar. **B** Ramus relationship of Pell&Gregory Classification. PG-I: Sufficient space available between the anterior border of the ascending ramus and distal side of second molar to accommodate mesiodistal width of the crown of the M3. PG-II: The space available between the anterior border of the ramus and the distal side of the second molar is less than the mesiodistal width of the crown of the M3. PG-III: All or most of the M3 is embedded in the mandibular ramus

Angle malocclusion classification, respectively. Group 1 was for male, Group 2 was for female, Group 3 was for class I malocclusion, Group 4 was for class III malocclusion, Group 5 was for 18–27 years old and Group 6 was for 28–40 years old.

Statistical analysis

The statistical analyses were performed on SPSS (version 27.0, IBM Co, Armonk, NY USA). All measurement work was done by the same researcher, and each measurement result was repeated 3 times, and the average value of the 3 measurement results was taken.

All data were given as mean \pm standard deviation (SD). Pearson correlation coefficient was used to analyze the correlations among the angle of line-line, line-plane. A paired t-test was performed to compare the measurement in left and right independent t-test was performed to compare the measurement in Group1 and 2, Group3

and 4, Group5 and 6. One-way ANOVA was performed to analyze RS differences between paired groups. Pairwise comparison between classifications was performed by LSD test. 95% confidence intervals were set for all statistical analyses ($P < 0.05$).

Results

Classification, number and corresponding patient age

Table 2 showed the classification and number of the M3. The number of each classification is similar. No statistically significant differences in corresponding age among the compared classifications were found, except for age in PG-I/II/III classification. The corresponding patient age in PG-I classification was the largest, followed by PG-II classification, and the smallest was PG-III classification ($P > 0.05$) (Table 2).

The correlation of FH-related angulations

For the face-face angle and the line-face angle, \angle FH-WP showed a strong correlation with \angle FH-WL ($r = 0.992$, $P < 0.05$), the corresponding standard deviation of the two were 3.73 and 3.74. \angle FH-OP showed a weak correlation with \angle FH-OL ($r = 0.332$, $P < 0.05$), the corresponding standard deviation of the two were 6.99 and 5.58. \angle FH-WP angle had strong correlations with the \angle FH-OP angle ($r = 0.619$, $P < 0.05$), \angle FH-WL angle was moderately correlated with the \angle FH-OL angle ($r = 0.475$, $P < 0.05$) (Table 3).

Differences of different groups of RS, A angle and B angle

RS decreased gradually from the crown to the root, and the minimum was at the root tip (4.39 ± 1.95 mm in WP group, 3.81 ± 1.54 mm in OP group). Significant statistical differences were found in the amount of RS between groups WP and OP, in all levels ($P < 0.05$). In the WP group, RS at the root level (level 3, 4, 5) was longer than in the OP group, and RS at the crown level (level 1, 2) was shorter. A, B angles had no statistical significance between two groups (Table 4). For all measurements, no statistical difference existed between the right and left sides (Table 4). Similarly, there was also no statistical difference in sex and Angle's classification. However, significant differences between different age groups in B angles and RS of level 5 were found ($P < 0.05$); Group 6 displayed larger measurements than Group 5 (Table 5).

Differences of RS across different third molars classifications

In the WP group, almost all RS had statistical differences in classification criteria of PG-A/B/C, PG-I/II/III and mesiodistal angulation ($P < 0.05$), except RS of level 2 in PG-I/II/III. However, no statistical difference between RS and B angle was found. In different Pell & Gregory

Table 2 Basic information of the third molars

| Classification criterion | Groups | Number | Corresponding age ^a | Corresponding gender | |
|--------------------------|----------------|--------|--------------------------------|----------------------|--------|
| | | | | male | female |
| Depth | PG-A | 85 | 29.08 ± 0.61 | 44 | 41 |
| | PG-B | 60 | 27.00 ± 0.76 | 29 | 32 |
| | PG-C | 61 | 28.82 ± 0.74 | 30 | 31 |
| | <i>P</i> Value | | 0.082 | | |
| Ramus Relationship | PG-I | 78 | 30.17 ± 0.65 | 41 | 37 |
| | PG-II | 75 | 28.41 ± 0.66 | 40 | 35 |
| | PG-III | 53 | 25.77 ± 0.70 | 21 | 32 |
| | <i>P</i> Value | | 0.000*** | | |
| Mesiodistal angle | A1 | 68 | 28.65 ± 0.67 | 31 | 37 |
| | A2 | 69 | 27.80 ± 0.76 | 37 | 32 |
| | A3 | 69 | 28.75 ± 0.68 | 34 | 35 |
| | <i>P</i> Value | | 0.573 | | |
| Labiolingual angle | B1 | 71 | 29.79 ± 0.59 | 37 | 34 |
| | B2 | 70 | 27.96 ± 0.69 | 36 | 34 |
| | B3 | 65 | 27.35 ± 0.80 | 29 | 36 |
| | <i>P</i> Value | | 0.056 | | |
| Total | <i>n</i> = 206 | 206 | 28.40 ± 0.40 | 102 | 104 |

^a One-way ANOVA of corresponding age in each three groups under different classification criteria

*** Significant difference at *P* < 0.05

Table 3 Pearson correlation coefficients of FH-related angulations

| Reference | Face-face angulations Mean ± SD (°) | Line-face angulations Mean ± SD (°) | <i>r</i> |
|-----------|--|--|----------|
| WP/WL | 11.50 ± 3.73(< FH-WP) | 11.53 ± 3.74(< FH-WL) | 0.992** |
| OP/OL | 1.84 ± 6.99(< FH-OP) | 10.30 ± 5.58(< FH-OL) | 0.332** |
| <i>r</i> | 0.619** | 0.475** | |

Pearson correlation coefficients was labeled bold; **Significant difference at *P* < 0.05

classifications, from PG-A to PG-C, PG-I to PG-III, a gradual decrease in RS was seen (*P* < 0.05). In mesiodistal angulation, from A1 to A3, RS showed an increasing trend (*P* < 0.05) (Table 6).

Discussion

Recent findings have shown RS is a three-dimensional spatial definition [10, 11]. The RS was analyzed in CBCTs to minimize measurement inaccuracies, such as the ones normally seen when utilizing conventional 2D radiographs [18]. This study aimed to use CBCT to reconstruct

a 3D model and test for an association between RS and third molar positional traits.

Patients we included were adults aged 18 to 40 years with non-vertical growth. Zhao Z et al. found RS had a maximum in the hypodivergent group and was twice as large as in the hyperdivergent group [19]. Research reports the missing rate of M3 in patients with vertical skeletal craniofacial pattern was higher, our patients were selected based on evidence found in the literature [20]. In the current study, we found that with the increase in average age, the M3 tends to PG-I within the classification of ramus relationship. Possibly as a result of the eruption of the M3 increases the eruption space and promotes the further growth of the mandibular angle [21].

In addition, previous studies used OP to measure the amount of tooth movement [10, 11, 19]. The tooth movement of malocclusion patients in orthodontic treatment is likely to influence the position of OP [22]. The findings confirmed the WALA ridge arch can represent the alveolar arch [23]. The dental arch and WALA ridge arch have high matching [24]. In this study, the distance from the WP plane fitted by least squares method to each point on WALA ridge arch has a minimum and the WALA ridge arch was fitted into a relatively stable plane to represent

Table 4 Comparison of data between groups in different levels

| RS of Level 1–5 (mm) | Group ^a of different references | | | Group ^b of different sides | | |
|----------------------|--|----------------|--------------|---------------------------------------|----------------|--------|
| | WP groups | OP groups | WP VS OP | Right (R) | Left (L) | R VS L |
| | Mean ± SD (mm) | Mean ± SD (mm) | P | Mean ± SD (mm) | Mean ± SD (mm) | P |
| L1 | 11.10 ± 2.30 | 11.49 ± 2.06 | 0.045 | 11.21 ± 2.11 | 11.39 ± 2.26 | 0.269 |
| L2 | 10.62 ± 1.81 | 11.17 ± 1.57 | 0.001 | 10.92 ± 1.72 | 10.87 ± 1.72 | 0.704 |
| L3 | 7.84 ± 1.87 | 7.02 ± 1.83 | 0.000 | 7.57 ± 1.86 | 7.24 ± 1.85 | 0.058 |
| L4 | 6.48 ± 1.84 | 5.43 ± 1.69 | 0.000 | 6.03 ± 1.88 | 5.82 ± 1.70 | 0.075 |
| L5 | 4.39 ± 1.95 | 3.81 ± 1.54 | 0.001 | 4.14 ± 1.63 | 3.98 ± 1.85 | 0.142 |
| A angle | 48.83 ± 32.57 | 41.85 ± 31.07 | 0.113 | 45.51 ± 32.35 | 43.17 ± 31.45 | 0.231 |
| B angle | 19.06 ± 15.07 | 16.63 ± 11.75 | 0.069 | 17.20 ± 14.47 | 18.50 ± 12.57 | 0.075 |

^a Two-samples independent t-test and test for normality was significant ($P < 0.05$), ^bA paired t-test and test for normality was significant ($P < 0.05$)
The significance level $P < 0.05$ was labeled bold

Table 5 Comparison of Measurements at Group1 and Group2, Group3 and Group4, Group5 and Group6^a

| Measurements (the RS of level and angle) | sex(N) | | | Angle's classification(N) | | | Age(N) | | |
|--|---------------|---------------|-------|---------------------------|---------------|-------|---------------|---------------|--------------|
| | Group1(208) | Group2(204) | P | Group3(332) | Group4(90) | P | Group5(216) | Group6(196) | P |
| | Mean ± SD | Mean ± SD | | Mean ± SD | Mean ± SD | | Mean ± SD | Mean ± SD | |
| L1 | 11.38 ± 2.30 | 11.22 ± 2.07 | 0.465 | 11.31 ± 2.21 | 11.27 ± 2.13 | 0.861 | 10.88 ± 2.26 | 11.36 ± 2.33 | 0.723 |
| L2 | 10.81 ± 1.92 | 10.98 ± 1.49 | 0.314 | 10.93 ± 1.72 | 10.76 ± 1.70 | 0.410 | 10.61 ± 1.71 | 10.63 ± 1.93 | 0.322 |
| L3 | 7.73 ± 1.88 | 7.13 ± 1.87 | 0.001 | 7.45 ± 1.89 | 7.37 ± 1.93 | 0.743 | 7.74 ± 1.77 | 7.95 ± 1.98 | 0.524 |
| L4 | 6.02 ± 1.76 | 5.89 ± 1.92 | 0.490 | 5.95 ± 1.85 | 5.95 ± 1.82 | 0.980 | 6.21 ± 1.81 | 6.78 ± 1.83 | 0.058 |
| L5 | 3.94 ± 1.82 | 4.26 ± 1.73 | 0.066 | 4.06 ± 1.78 | 4.23 ± 1.77 | 0.425 | 3.97 ± 1.87 | 4.85 ± 1.95 | 0.000 |
| A angle | 43.61 ± 31.78 | 45.06 ± 32.06 | 0.645 | 44.35 ± 31.37 | 44.31 ± 33.88 | 0.990 | 45.72 ± 32.04 | 48.06 ± 33.27 | 0.541 |
| B angle | 17.30 ± 13.49 | 18.39 ± 13.62 | 0.418 | 17.96 ± 14.37 | 17.45 ± 10.13 | 0.704 | 16.10 ± 14.30 | 21.75 ± 15.31 | 0.000 |

^a Independent sample T-test of measured values under different genders, different Angle's classification, and different ages
The significance level $P < 0.05$ was labeled bold

the bony alveolar arch plane, namely the WP plane [25]. Hence, this study fitted the WP as a reference plane. It was also the innovation of this study. We found that WP had high stability in the present study by comparing the standard deviation of <FH-WP and <FH-OP. It is suggesting that WP can be the reference plane. WL and WP were highly correlated and the result was supported by Gupta [24]. This may reflect the fact that the selected measurement datum line is also scientific. In our study, the OP was used as an auxiliary to illustrate the reliability of the results obtained by the WP.

In recent years, three-dimensional digital technology with high efficiency, high accuracy, and high maneuverability can help dentists to simulate orthognathic surgery, three-dimensionally reconstruct the airway structure, analyze organizational change in orthodontic treatment and provide effective means for personalized orthodontic treatment [26]. With the development of digital orthodontics, digital models as well as invisible and personalized appliances have been widely used. In this study, digital technology was also used to fit the plane, which

is an innovative method, hoping to help the follow-up orthodontic research work.

Because of a certain angle between the reference planes, it had noticeable differences in RS which were obtained by OP and WP in this study. The consistent results with Kim were that RS at the crown level was longer than at the root level and RS had a gradual reduction from the crown to the root tip [10]. Thus, the distally-induced movement of roots is a clinical procedure that merits concern. During distal movement, the molars will tilt when the root tip touches the cortical bone. This is consistent with many previous studies [2728]. Otherwise, RS had no significant difference in gender and Angle's classification. In the age classification, the older group has larger RS (especially in the root tip) and B angle. The finding by Choi [11] that the available space at the posterior boundary of molars is influenced by age supports our results. From this, the influence of age on RS should be considered in orthodontics. The influence of age on RS may be caused by periodontal disease or physiological alveolar ridge absorption [29].

Table 6 Comparison of RS under different classifications of the third molars in WP groups^a

| Classification criterion | Classification | The RS of Level 1–5(mm) | | | | |
|--------------------------|----------------|-------------------------|--------------|--------------|--------------|--------------|
| | | L1 | L2 | L3 | L4 | L5 |
| Depth | PG-A | 12.55 ± 1.86 | 10.74 ± 1.68 | 8.51 ± 1.67 | 6.94 ± 1.72 | 5.01 ± 1.77 |
| | PG-B | 10.95 ± 1.87 | 11.04 ± 1.68 | 7.87 ± 1.63 | 6.11 ± 1.92 | 4.19 ± 2.07 |
| | PG-C | 9.25 ± 1.83 | 10.03 ± 1.99 | 6.86 ± 1.96 | 6.19 ± 1.79 | 3.7 ± 1.81 |
| | P Value | 0.000 | 0.006 | 0.009 | 0.000 | 0.000 |
| Ramus Relationship | PG-I | 12.51 ± 1.87 | 10.88 ± 1.91 | 8.61 ± 1.61 | 7.26 ± 1.73 | 5.22 ± 1.87 |
| | PG-II | 10.83 ± 2.05 | 10.60 ± 1.70 | 7.66 ± 1.92 | 6.32 ± 1.81 | 4.28 ± 1.75 |
| | PG-III | 9.44 ± 1.94 | 10.24 ± 1.78 | 6.94 ± 1.73 | 5.56 ± 1.57 | 3.33 ± 1.80 |
| | P Value | 0.000 | 0.144 | 0.000 | 0.000 | 0.000 |
| Mesiodistal angle | A1 | 9.38 ± 1.86 | 9.95 ± 1.68 | 7.51 ± 2.02 | 6.52 ± 1.99 | 4.15 ± 1.98 |
| | A2 | 11.03 ± 1.94 | 10.6 ± 1.88 | 7.51 ± 1.76 | 6.06 ± 1.79 | 4.09 ± 1.99 |
| | A3 | 12.89 ± 1.57 | 11.15 ± 1.65 | 8.49 ± 1.67 | 6.85 ± 1.65 | 4.93 ± 1.79 |
| | P Value | 0.000 | 0.000 | 0.002 | 0.037 | 0.018 |
| Labiolingual angle | B1 | 10.81 ± 2.38 | 10.68 ± 1.89 | 8.17 ± 1.71 | 6.95 ± 1.78 | 4.51 ± 2.06 |
| | B2 | 11.28 ± 2.39 | 10.61 ± 1.67 | 7.79 ± 1.91 | 6.33 ± 2.00 | 4.34 ± 2.15 |
| | B3 | 11.24 ± 2.11 | 10.54 ± 1.90 | 7.52 ± 1.87 | 6.12 ± 1.60 | 4.30 ± 1.58 |
| | P Value | 0.406 | 0.911 | 0.127 | 0.051 | 0.804 |

^a ANOVA of RS in each three groups under different classification criteria

The significance level $P < 0.05$ was labeled bold

The connection between M3 and RS is controversial. Previous studies [11, 19] analyzed the RS with or without the M3 and found no notable difference. However, previous studies reported that the existence of the M3 would increase the available space of the posterior segment of the dental arch [30]. But these scholars did not classify M3s in detail. Therefore, this study conducted an in-depth classification study and found that RS was significantly different across distinct classifications. In Pell-Gregory classifications, the RS presented a gradual reduction from PG-A to PG-C. Similarly, RS gradually decreased from PG-I to PG-III. With respect to angle classification, the smaller the A angle is, the shorter is the RS. No significant difference existed in the B angle classification. In this study, we also confirmed significant differences in the mesial tilt degree of M3 in PG-A/B/C and PG-I/II/III classification. B angle has no significant difference across Pell-Gregory classifications. In agreement with our results, Tsai H confirmed that posterior molar space was related to the M3 mesial angle [31]. Consequently, an association indeed exists between RS and M3 depth, the degree of mesial tilt and the distance between the anterior edge of mandibular ramus and the second molar. RS can be initially estimated by observing the depth, mesial angle, or posterior space of M3. Our

findings could be used to help some primary hospitals without large dental facilities predict RS by observing panoramic or lateral radiograph, which will be beneficial to the design of orthodontic plans to induce molar distalization.

Finally, I want to summarize the main data of this study. A strong correlation ($r = 0.992$) between \angle FH-WP and \angle FH-WL. A strong correlation ($r = 0.619$) between \angle FH-WP angle and \angle FH-OP angle, too. Rs has a minimum value of 4.39 ± 1.95 mm at the root tip in WP group. Comparison results of variance analysis of RS under different M3 classifications: $P < 0.05$ in Pell & Gregory classifications and mesiodistal angulation classification.

Conclusions

1. Compared with the occlusal plane, the fitting WALA ridge plane had higher stability; the fitting WALA ridge plane can be used as an innovative plane for orthodontic clinical scientific research.

2. The retromolar space at crown level was longer than at the root level, and only minimally present at the root apex. Therefore, special attention should be paid to the initial retromolar space at the apical level when inducing molar distalization.

3. The current study found that retromolar space was significantly different across distinct positional traits of the mandibular M3. These M3 positional traits can be observed before orthodontics to predict the amounts of molar distalization.

Abbreviations

| | |
|------|--------------------------------|
| 3D | Three-dimensional |
| CBCT | Cone-beam computed tomography |
| RS | Retromolar space |
| M3 | The mandibular third molars |
| WP | The fitting WALA ridge plane |
| OP | The occlusal plane |
| FH | The Frankfort horizontal plane |
| WL | The WALA ridge line |
| OL | The occlusion line |
| MD | Molar distalization |
| SD | Standard deviation |
| MC | Mandibular canal |

Acknowledgements

Not applicable

Authors' contributions

Yumei Huang contributed to conception, design, data acquisition, analysis, and interpretation, drafted and critically revised the manuscript. Yunjia Chen, Dan Yang, and Yingying Tang contributed to data collection interpretation. Other authors contributed to revise the manuscript. All authors have read and approved the manuscript.

Funding

Project Supported by Chongqing Talent Program: Innovative leading talents (Medical field, CQYC20210303384). Chongqing Medical Scientific Research Project (2018ZDXM020).

Availability of data and materials

The datasets generated or analysed during the current study are available from the corresponding author on reasonable request.

Declarations

Ethics approval and consent to participate

All the research work has been carried out in accordance with The Code of Ethics of the World Medical Association (Declaration of Helsinki). All patients involved in this study had provided the written informed consent. The study was approved by the Research and Ethics Committee of the Affiliated Stomatology Hospital of Chongqing Medical University.

Consent for publication

Not applicable.

Competing interests

The authors declare no competing of interest.

Author details

¹Stomatological Hospital of Chongqing Medical University, Chongqing, China. ²Chongqing Key Laboratory of Oral Diseases and Biomedical Sciences, Chongqing, China. ³Chongqing Municipal Key Laboratory of Oral Biomedical Engineering of Higher Education, Chongqing, China.

Received: 7 July 2022 Accepted: 27 February 2023

Published online: 10 March 2023

References

- Janson G, Goizueta OEFM, Garib DG, et al. Relationship between maxillary and mandibular base lengths and dental crowding in patients with complete Class II malocclusions. *Angle Orthod*. 2011;81(2):217–21.
- Robertson L, Kaur H, Fagundes NCF, et al. Effectiveness of clear aligner therapy for orthodontic treatment: a systematic review. *Orthod Craniofacial Res*. 2020;23(2):133–42.
- Hong K, Kim WH, Eghan-Acquah E, et al. Efficient Design of a Clear Aligner Attachment to Induce Bodily Tooth Movement in Orthodontic Treatment Using Finite Element Analysis. *Materials*. 2021;14(17):4926.
- Nguyen M P. Evaluation of Dental and Skeletal Changes with Sequential Distalization of Maxillary Molars Using Clear Aligners: A preliminary study. West Virginia University; 2021.
- Papadimitriou A, Mousoulea S, Gkantidis N, et al. Clinical effectiveness of Invisalign® orthodontic treatment: a systematic review. *Prog Orthod*. 2018;19(1):1–24.
- 박가영. Posterior anatomic limit for distalization of maxillary dentition. Seoul, Yonsei University. 2020.
- Ye JA, Tsai CY, Lee YH, et al. Could cephalometric landmarks serve as boundaries of maxillary molar distalization? A comparison between two- and three-dimensional assessments. *Taiwan J Orthodont*. 2021;33(3):1.
- Bayome M, Park JH, Bay C, et al. Distalization of maxillary molars using temporary skeletal anchorage devices: A systematic review and meta-analysis. *Orthod Craniofacial Res*. 2021;24:103–12.
- Ravera S, Castroflorio T, Garino F, et al. Maxillary molar distalization with aligners in adult patients: a multicenter retrospective study. *Prog Orthod*. 2016;17(1):1–9.
- Kim SJ, Choi TH, Baik HS, et al. Mandibular posterior anatomic limit for molar distalization. *Am J Orthod Dentofacial Orthop*. 2014;146(2):190–7.
- Choi YT, Kim YJ, Yang KS, et al. Bone availability for mandibular molar distalization in adults with mandibular prognathism. *Angle Orthod*. 2018;88(1):52–7.
- Sohal KS, Moshy JR, Owibingire SS, et al. Association between impacted mandibular third molar and occurrence of mandibular angle fracture: a radiological study. *J Oral Maxillofacial Radiol*. 2019;7(2):25.
- Susarla SM, Dodson TB. Risk factors for third molar extraction difficulty. *J Oral Maxillofacial Surg*. 2004;62(11):1363–71.
- Yumei H, Yun H, Leilei Z. A study of the correlation between the digitally fitted WALA ridge plane and the mandibular body axial plane and occlusion plane. *J Practical Stomatol*. 2022;38(3):373–8.
- Marchiori DF, Packota GV, Boughner JC. Third-molar mineralization as a function of available retromolar space. *Acta Odontol Scand*. 2016;74(7):509–17.
- Padhye MN, Dabir AV, Girotra CS, et al. Pattern of mandibular third molar impaction in the Indian population: a retrospective clinico-radiographic survey. *Oral Surg Oral Medicine Oral Pathol Oral Radiol*. 2013;116(3):e161–6.
- Zeynep Gümrükü, Balaban E, Karaba M. Is there a relationship between third-molar impaction types and the dimensional/angular measurement values of posterior mandible according to Pell & Gregory/Winter Classification? *Oral Radiology*. 2020;37(1):1–7.
- Noffke CEE, Nzima N, Farman AG. Guidelines for the safe use of dental and maxillofacial CBCT: a review with recommendations for South Africa. *South African Dental J*. 2011;66(6):262–6.
- Zhao Z, Wang Q, Yi P, et al. Quantitative evaluation of retromolar space in adults with different vertical facial types: Cone-beam computed tomography study. *Angle Orthod*. 2020;90(6):857–65.
- Huang Y, Yan Y, Cao J, et al. Observations on association between third molar agenesis and craniofacial morphology. *J Orofacial Orthopedics/ Fortschritt der Kieferorthopädie*. 2017;78(6):504–10.
- Marchiori DF, Packota GV, Boughner JC. Initial third molar development is delayed in jaws with short distal space: An early impaction sign? *Arch Oral Biol*. 2019;106: 104475.
- Serafin M, Fastuca R, Castellani E, et al. Occlusal plane changes after molar distalization with a pendulum appliance in growing patients with class II malocclusion: a retrospective cephalometric study. *Turk J Orthod*. 2021;34(1):10.
- Glass TR, Tremont T, Martin CA, et al. A CBCT evaluation of root position in bone, long axis inclination and relationship to the WALA Ridge/Seminars in Orthodontics. *WB Saunders*. 2019;25(1):24–35.

24. Shu R, Han X, Wang Y, et al. Comparison of arch width, alveolar width and buccolingual inclination of teeth between Class II division 1 malocclusion and Class I occlusion. *Angle Orthod.* 2013;83(2):246–52.
25. Schomaker V, Waser J, Marsh RE, et al. To fit a plane or a line to a set of points by least squares. *Acta Crystallogr A.* 1959;12(8):600–4.
26. Gross D, Gross K, Wilhelmy S. Digitalization in dentistry: ethical challenges and implications. *Quintessence Int.* 2019;50(10):830.
27. Sugawara J, Kanzaki R, Takahashi I, et al. Distal movement of maxillary molars in nongrowing patients with the skeletal anchorage system. *Am J Orthod Dentofacial Orthop.* 2006;129(6):723–33.
28. Kook YA, Park JH, Bayome M, et al. Distalization of the mandibular dentition with a ramal plate for skeletal Class III malocclusion correction. *Am J Orthod Dentofacial Orthop.* 2016;150(2):364–77.
29. Sapey E, Yonel Z, Edgar R, et al. The clinical and inflammatory relationships between periodontitis and chronic obstructive pulmonary disease. *J Clin Periodontol.* 2020;47(9):1040–52.
30. Ghougassian SS, Ghafari JG. Association between mandibular third molar formation and retromolar space. *Angle Orthod.* 2014;84(6):946–50.
31. Tsai HH. Factors associated with mandibular third molar eruption and impaction. *J Clin Pediatr Dentist.* 2005;30(2):109–13.

Publisher's Note

Springer Nature remains neutral with regard to jurisdictional claims in published maps and institutional affiliations.

Ready to submit your research? Choose BMC and benefit from:

- fast, convenient online submission
- thorough peer review by experienced researchers in your field
- rapid publication on acceptance
- support for research data, including large and complex data types
- gold Open Access which fosters wider collaboration and increased citations
- maximum visibility for your research: over 100M website views per year

At BMC, research is always in progress.

Learn more biomedcentral.com/submissions

